

Letter to the Editor Concerning “Direct Spectroscopic Evidence of Magnetic Proximity Effect in MoS₂ Monolayer on Graphene/Co”

Elena Voloshina,^{*,†,‡,¶} Na Zhu,[†] Jiaxin Zhang,[†] Beate Paulus,[‡] and
Yuriy Dedkov^{*,†,§}

[†]*Department of Physics, Shanghai University, 99 Shangda Road,
200444 Shanghai, P. R. China*

[‡]*Institut für Chemie und Biochemie, Freie Universität Berlin, Arnimallee 22,
14195 Berlin, Germany*

[¶]*Present Address: Ruđer Bošković Institute, Division of Theoretical Physics,
Bijenička cesta 54, 10000 Zagreb, Croatia*

[§]*Present Address: Center for Advanced Laser Techniques, Institute of Physics,
Bijenička cesta 46, 10000 Zagreb, Croatia*

E-mail: elena.voloshina@icloud.com; yuriy.dedkov@icloud.com

Abstract

Recently, the electronic and magnetic properties of the MoS₂-graphene van der Waals heterostructure epitaxially grown on ferromagnetic Co(0001) were investigated using different experimental methods accompanied by density functional theory (DFT) calculations [Voroshnin et al., *ACS Nano* **2022**, 16, 7448]. Despite the large distance

between the S-terminated Co(0001) surface and Mo atoms of $\approx 7.6 - 9.8 \text{ \AA}$ (depending on the system's model), a sizeable magnetically induced exchange spin-splitting of $\approx 20 \text{ meV}$ for the MoS₂-derived valence band states at the Γ point was found and supported by the DFT calculations. Our present realistic state-of-the-art large-scale DFT calculations performed for different MoS₂-graphene-Co interfaces (with and without inclusion of interface S atoms) rule out such effect and the possibility to induce any sizeable magnetic moment in the MoS₂ layer and the respective spin-splitting of the MoS₂-derived bands. It is explained by the large distances between Mo and Co atoms in all considered cases and that magnetic interaction between them is screened by S and C layers in the studied systems.

Transition metal dichalcogenides (TMDs), the class of 2D materials with a structural formula MX₂, recently attracted an increased attention because of the possible applications of these layered materials in different areas ranging from catalysis and sensing to optospintronics.¹⁻⁶ In case of MoS₂, which is a representative example in this class of materials, with a band gap of 1.8 eV, two spin-orbit split valleys at the K and K' points have opposite spins⁷ that can be detected either in circular dichroism experiments or using spin-resolved photoelectron spectroscopy.⁸⁻¹² Several ways to control spin-polarization of the respective spin-orbit split states at K and K' were proposed, like external magnetic field,¹³⁻¹⁵ magnetic impurities in single- or multilayer MoS₂,^{16,17} defects engineering^{18,19} or via proximity with ferromagnetic or antiferromagnetic materials.²⁰⁻²² In the later case of the MoS₂/YIG system (YIG is the yttrium iron garnet magnetic insulator), it was found that the magnetic proximity effect disappears at distances more than 5 \AA with antiferromagnetic coupling at the interface between two materials.²⁰ The effective charge transfer of spin-polarized electrons was found, however without hybridization of the electronic states at the interface.

Recently, several experimental works appeared in the literature, which aimed in the controllable epitaxial growth of TMDs layers on metals, like Au(111),^{23,24} or insulating substrates, like sapphire.²⁵ Further works demonstrated the successful decoupling of TMDs,

particularly of MoS₂ from metallic substrates using graphene (gr) as an intermediate layer.²⁶ The similar approach was suggested for the growth of MoS₂ on graphene prepared on ferromagnetic Co.²⁷ In this work the CVD grown gr/Co(0001) system was used as a support for the deposition of Mo layer and then the sulphurization of this layer at 600° C should lead to the formation of MoS₂ on gr/Co(0001). Despite the simultaneous intercalation of S-atoms in the gr/Co interface during formation of MoS₂, as confirmed by the respective angle-resolved photoelectron spectroscopy (ARPES) experiments, and the large distance of $\approx 8 - 9 \text{ \AA}$ between magnetically dead Co interface atoms and Mo atoms, which are magnetically screened from Co by graphene layer and S-atoms, the sizeable exchange spin splitting of the MoS₂ energy bands at the Γ point of $\approx 20 \text{ meV}$ is found at room temperature, confirmed also by the density functional theory (DFT) calculations. If one assumes that the same empirical rule for the magnetic moment of 3d metals (1 eV of the exchange splitting of the 3d states near the Fermi level approximately corresponds to the $1 \mu_B$ of the local magnetic moment)^{28,29} is also valid for the magnetic state of 4d atoms, then the induced magnetic moment of $0.02 \mu_B/\text{Mo-atom}$ is expected for MoS₂ grown on gr/Co(0001) substrate. Such results lead to the estimation of the effective magnetic field produced by the gr/Co substrate of $\sim 100 \text{ T}$. The obtained values for the magnetic moment in MoS₂ are comparable to the induced magnetic moment of carbon atoms in graphene ($0.05 - 0.1 \mu_B$), which, however, was found in much closer proximity to ferromagnetic Ni, Fe or Co at the distance of $\approx 2 \text{ \AA}$, where the effective hybridization of the electronic states and charge transfer at the interface were found.³⁰⁻³² Therefore, the systematic studies and analysis of the observed effects for the MoS₂/gr/Co(0001) system where interaction between layers is of the van der Waals origin are required in order to shed more light on the mechanism causing the respective observed magnetic phenomena.

Here, we present systematic realistic large-scale DFT studies of different layered systems combining MoS₂ and graphene layers on ferromagnetic Co(0001). In order to correctly describe the complete set of experimental data (observed *p*-doping of a graphene layer),

we considered large-scale epitaxial systems corresponding to the respective periodicities of the MoS₂ and graphene layers, and additionally the effect of intercalated S-atoms in the gr/Co(0001) interface with distributed S-atoms or formation of the CoS_x layer was taken into account. Our results unequivocally demonstrate that, taking into account all experimental observations, only MoS₂/gr on S^{int}/Co(0001) correctly reproduces the obtained results. It is also demonstrated that in all considered cases the exchange spin splitting of energy bands and induced magnetic moment in MoS₂ are absent and not reproduced in realistic DFT calculations. The absence of the claimed effects is clearly explained by the van der Waals origin of interactions in the considered systems at the large distances between weakly coupled graphene and MoS₂ layers, and by the screening effect caused by graphene and S atoms for the strongly reduced magnetic moments of the interface Co atoms. The presented results point to the importance of the careful analysis of the presented experimental data, which might be of importance for further studies of different layered heterostructures.

Discussion of observations by Voroshnin et al. [Ref. 27]

Before presenting our systematic and realistic large-scale DFT studies of different systems which combine MoS₂, graphene and Co(0001), we would like to point to several critical questions that cast doubt on the results presented in the article by Voroshnin et al.²⁷

- Let us firstly compare ARPES and spin-resolved photoemission data presented in two figures from the article by Voroshnin et al.:²⁷ Fig. 2a and Fig. 3, respectively. As it is well known and clearly stated in Ref. 27: “The band structure of MoS₂ depends on the number of layers: in a few-layer stack, the valence-band maximum is located at the $\bar{\Gamma}$ point, while in a single-layer it is at \bar{K} . Figure 2a shows that the valence-band maximum is at the \bar{K} point, demonstrating that the MoS₂ film is one monolayer thick.” This is true for Fig. 2a of Ref. 27 and one can see that the position of the band at the $\bar{\Gamma}$ point is by ≈ 250 meV lower compared to the band position of the upper spin-orbit-

split band at the \bar{K} point. However, if we compare the positions of these bands in Fig. 3 of Ref. 27 then we can see that these bands have the same binding energies, thus contradicting to Fig. 2a and to the statement in the manuscript.

- According to the article by Voroshnin et al.,²⁷ the coverage of MoS₂ in the synthesised trilayer is about 0.4 ML. Therefore, the apparent “spin splitting of MoS₂ states” may actually be the spin-polarised signal, which comes from the graphene/Co(0001) support underneath MoS₂. Particularly it can happen for the photon energy of 20 eV, which was used for the spin-resolved photoemission experiments. At this photon energy, the photoemission cross section for the Mo 4*d* and S 3*p* valence band states is larger compared to the value for Co 3*d* by factor of ≈ 6 and ≈ 1.5 , respectively. However, in the photoemission experiments this difference is partly compensated by the non-complete coverage for the MoS₂ layer, that leaves some parts of the gr/Co(0001) support naked to the light. In this case the contribution of the spin-polarized photoemission signal, which originates from the gr/Co(0001) support, to the total photoemission picture is expected to be very significant. The evidence that the background photoemission signal from gr/Co(0001) is spin-polarised is the shift of two curves, spin-up and spin-down, in vertical direction in Fig. 3a,c,e of Ref. 27 and the spin-polarized (or spin-split) intensity “bump” clearly visible at 0.9 eV in Fig. 3a Ref. 27. Moreover, the previous spin-resolved photoemission data for gr/Co(0001) measured at the Γ point clearly demonstrate the strong variation of the spin polarization (in value and in sign) in the range of 2 eV below the Fermi level,³³ i. e. exactly in the energy range where spin-resolved experiments for MoS₂ on gr/Co(0001) are presented in Ref. 27. [The photon energy used in Ref. 33 is different from the one used in the discussed work.²⁷ However, taking into account the band structure of gr/Co(0001) the similar strong variation of the spin-polarization is expected.] Unfortunately, such reference spin-resolved photoemission at photon energy of 20 eV for the gr/Co(0001) system are not presented in Ref. 27. Therefore without such reference data one cannot unequivocally claim that presented spin-splitting ob-

served for the MoS₂-derived states is due to the intrinsic spin-polarisation of the MoS₂ states. Moreover, using the parameters which can be considered as very close to the real ones used in the discussed experiment,²⁷ we present the very rough example of how the spin-splitting in the background signal (with spin splitting of 1 eV) can introduce the “spin-splitting” of 30 meV for the band which is not originally spin-polarized (Fig. 1). Here, spin-up and spin-down Lorentzians simulate the photoemission intensity from the respective exchange-split states of the ferromagnetic substrate. If we compare data in Fig. 3a of Ref. 27 and Fig. 1 of the present work, we can clearly see that the claimed effect is clearly reproduced; however, without intrinsic spin-polarization for the initially non spin-polarized emission line. These simulations do not pretend on the completeness and cannot be considered as an attempt to simulate the experimental data presented in Ref. 27, but they point on the importance of preliminary reference data for gr/Co(0001) (used as a support for the MoS₂ growth), which are unfortunately missed in the original work.

- Here we also would like to note that in Ref. 27 the energy resolution of 10 meV and 45 meV are claimed for ARPES and spin-resolved ARPES experiments at room temperature, respectively. However, the dominant factor in such experiments is the thermal broadening caused by the sample’s temperature and which amounts to $\Delta E \approx 4k_B T \approx 120 \text{ meV}$,³⁴ which is much large compared to the claimed exchange spin splitting of 20 meV for the MoS₂-derived band at the Γ point and claimed energy resolutions.
- In manuscript of Voroshnin et al.²⁷ the crystallographic structure of the resulting system for which ARPES and spin-resolved photoemission data are presented do not correspond to the crystallographic structures which were used for the interpretation of spin-resolved photoemission data and in the DFT calculations. Moreover, only one model was used in the DFT calculations ignoring other possibilities as discussed below in section “Results and discussion”.

For example, in Ref. 27, the authors stay: “We relate it to the formation of a surface cobalt sulfide (CoS_x) under graphene.”, when considering LEED patterns, and “These domains demonstrate striped patterns, which are caused by underlying CoS_x .”, when considering the STM images. However, despite the experimental observations, the intercalation of S and the respective formation of CoS_x was not considered during interfaces modelling in Ref. 27. As it is shown below, the intercalation of S atoms in the gr/Co(0001) interface and formation of the CoS_x layer have a very strong implications on the electronic and magnetic properties of considered systems.

In Ref. 27, the authors mention: “A closer look at the region near the \bar{K} point [Figure 2c,e] reveals that graphene is slightly p-doped with the Dirac point located 0.3 eV above the Fermi level. We relate the doping to sulfur intercalation, as supported by additional experiments on sulfur-intercalated graphene/Co samples in the absence of MoS_2 [see Supporting Information, Figure S2].” Thus, the sulfur intercalation was presumed; however, it was fully ignored in further considerations when constructing the structural model for the theory part. From the theoretical data presented in Ref. 27 it is not clear if the linear dispersion of the graphene-derived π -bands, observed in the ARPES experiments, is maintained in the DFT calculations. Unfortunately, in Ref. 27 only very small portion of the electronic structure of very complicated system around some bands showing desired splitting is presented, not allowing to make clear conclusions about correct description of all effects observed in the experiment.

- The authors of Ref. 27 use very thin Co-slab of only 4 ML. This is an insufficient thickness in general, which is also very critical when working with magnetic systems. However, even more serious is the lack of passivation of the bottom layer of the slab by ad-atoms. The approach where the bottom layer of the thin metallic slab is passivated with ad-atoms, such as H or Al, is a common practice in computation materials modelling. This is especially important for consideration of spin-orbit related and exchange-splitting effects because of the inversion-symmetry breaking necessary in this

case.^{35,36} Also such layers protect the magnetic exchange interaction between slabs which can cause artefacts in the calculations. In our work we have performed the calculations for the $(4 \times 4)\text{MoS}_2/(5 \times 5)\text{graphene}/\text{Co}(0001)$ with the distances reported by Voroshnin et al.²⁷ with and without Al-passivation. The results of these calculations allow us to conclude that the claimed in Ref. 27 spin-splitting of the MoS_2 -derived states at the Γ point is an artefact due to the wrong computational approach (see discussion below and section “Methods”).

In our work, we eliminated the above-mentioned shortcomings of the theoretical part of the research carried out by the authors of Ref. 27:

- We are considering supercell that has the periodicity that was observed in the experiment, namely: a (9×9) lateral periodicity with respect to graphene and $\text{Co}(0001)$ and a (7×7) lateral periodicity with respect to MoS_2 (the resulting structure in our manuscript is approximately four times larger as compared to the model used in manuscript of Voroshnin et al.). This way the lattice mismatch of both two-dimensional materials, graphene and MoS_2 , is less than 1%. In our work, the slabs have sufficient thickness with the bottom side of each slab is protected by a layer of ad-atoms.
- Taking into account the synthesis conditions and experimental observations, we take into account the possible intercalation of S and the formation of CoS_x . This results in the consideration of 6 possible structures (instead of 1 random structure, which does not correspond to the experimental situation, investigated by Voroshnin et al.).
- We use the same code (see section “Methods”) for the structure optimization and for calculating the band structures. For each structure, all calculated parameters are extracted from the same output-file. Furthermore, we present all computational details so that the results can be clearly reproduced by any qualified reader.
- We disclose all our results: We present the optimised structures (see Supporting Information), optimized distances (see section “Results and discussion”), calculated band

structures in the ranges where graphene- and MoS₂-valence band states are visible (see section “Results and discussion”).

Results and discussion

The DFT optimized crystallographic structures of all systems studied in the present work are shown in Figure 2 and 3 (top and side views). On the first step, the spin-resolved electronic structure of the parent gr/Co(0001) interface, which was used in Ref. 27 as a substrate for the MoS₂ formation, is shown in Figure 3(c). In agreement with previous results^{37–39} graphene is adsorbed on Co(0001) in the so-called *top-fcc* configuration with a mean distance between Co top layer and graphene of 2.09 Å (one carbon atom of the graphene unit cell is adsorbed above the Co interface atom and second carbon atom is located at the *fcc* hollow site of the Co(0001) surface, see Fig. 3(a,b)). Due to the close proximity of graphene to the ferromagnetic Co(0001) surface, the characteristic linear dispersion of the graphene-derived π band is fully destroyed at the Fermi level.⁴⁰ In this situation the strong hybridization between graphene π and Co 3*d* states leads to the large band gap between π and π^* bands at the K point and formation of a series of the so-called hybrid interface states (Fig. 3(c)). As a result of the interface hybridization the magnetic moment in graphene is induced: $m(C^{top}) = -0.042 \mu_B$ and $m(C^{fcc}) = 0.038 \mu_B$, respectively (Tab. 1). At the same time the magnetic moment of Co(S) atoms is decreased to $1.514 \mu_B$ compared to the value of $1.707 \mu_B$ for the clean Co(0001) surface. [The magnetic moment inside the Co-slab is $1.579 \mu_B$.]

In Ref. 27 the MoS₂ layer was formed via sulphurization of the 1/3 ML-thick pre-deposited Mo-layer on top of gr/Co(0001) at the sulphur partial pressure of 5×10^{-9} mbar and substrate temperature of 600° C. Taking into account a large amount of experimental and theoretical works on the temperature-promoted interaction of the gr/metal interfaces with different species,^{41,42} the intercalation of sulphur atoms and/or Mo atoms in the gr/Co(0001) interface with the simultaneous formation of MoS₂ cannot be ruled out. Indeed, the intercalation of

S in gr/Co(0001) and formation of the gr-S interface is confirmed in Ref. 27 using XPS and via the observation of the restored linear dispersion of the graphene π bands and p -doping of graphene with the position of the Dirac point at $E - E_F \approx 0.3$ eV above the Fermi level. At the same time the complete undistorted band structure of the MoS₂ single layer is observed in ARPES experiments. Following these results, in order to fully understand the electronic and magnetic properties of the formed system, several interfaces have to be considered, where MoS₂/gr stack (in different order) can be formed on (i) clean Co(0001), (ii) CoS_{*x*}/Co(0001), or S/Co(0001) (Tab. 2). Also for the correct theoretical description of the formed system the full set of experimental data have to be taken into account. In the DFT analysis, which is presented below for all possible structures, due to the different number of atoms in the considered systems, the more energetically favourable structure (geometry) can only be concluded from the comparison of the total energies for the corresponding pairs, e. g. for gr/MoS₂/Co and MoS₂/gr/Co, etc.

Band structures calculated for the MoS₂/gr/Co(0001) and gr/MoS₂/Co(0001) systems are presented in Fig. 4(a,b), respectively, for graphene π and MoS₂ bands after unfolding procedure for the corresponding hexagonal Brillouin zone. The formation of the gr/MoS₂/Co(0001) system is more energetically favourable with the total energy gain of ≈ 9 eV (or ≈ 11 meV per atom) (Tab. 2). However, the formation of both systems in the described experiment²⁷ can be clearly ruled out: for MoS₂/gr/Co(0001) the linear dispersion of the graphene π band is not reproduced in the DFT calculations (Fig. 4(a)) and the obtained band structure is the same as for gr/Co(0001); for gr/MoS₂/Co(0001) the free-standing-like band structure of MoS₂ is completely lifted out indicating the strong hybridization of the electronic states at the MoS₂/Co interfaces and the obtained doping level of graphene on MoS₂/Co does not reproduce the experimental value ($E - E_F = 0.02$ eV in the DFT calculations vs. $E - E_F = 0.3$ eV in experiment). The calculated exchange spin-splitting of the MoS₂-derived states at the Γ point for the MoS₂/gr/Co(0001) system is 5 meV which is equal to the energy error of the unfolding procedure for such big system. This value is negligible

compared to the experimentally observed spin-splitting of 20 meV (at room temperature used in the experiment) and correlates with extremely small value of $0.002 \mu_B$ for the calculated magnetic moment of Mo atoms in MoS₂ (Tab. 2). These small values (if any) of the exchange spin-splitting and magnetic moments are due to the large gr-S, Co-S, and Co-Mo distances of 3.312 Å, 5.404 Å, and 6.960 Å, respectively, accompanied by the screening effect of the graphene layer, that prevents the effective electronic and magnetic exchange between Co and MoS₂ in the MoS₂/gr/Co(0001) system. The sizeable magnetic moments for Mo and S atoms in the MoS₂ layer of $0.011 \mu_B$ and $0.020 \mu_B$, respectively, are calculated for gr/MoS₂/Co(0001) with a close proximity between MoS₂ and Co layers. However, the formation of this system is not confirmed in the experiment (see above).

Further improvements of the obtained results with taking into account the more realistic experimental conditions when S-atoms are intercalated in the gr-Co or MoS₂-Co interfaces and form the CoS_x alloy (see Fig. 2(c,d)) lead to the results shown in Fig. 4(c,d) for MoS₂/gr/CoS_x/Co(0001) and gr/MoS₂/CoS_x/Co(0001) interfaces, respectively. The formation of the later system is more energetically favourable with the total energy gain of ≈ 11 eV (or ≈ 14 meV per atom) (Tab. 2). However, the similar conclusions on the electronic and magnetic properties of the graphene and MoS₂ layers can be also made in the present cases. First of all, the formation of the CoS_x alloy leads to the further reduction of the Co-atoms' magnetic moments to $1.509 \mu_B$ and $1.316 \mu_B$ for MoS₂/gr/CoS_x/Co and gr/MoS₂/CoS_x/Co, respectively. At the same time, the magnetic moments of Mo/S atoms in the MoS₂ layers for the considered systems are $0.003/0.000 \mu_B$ and $-0.007/0.012 \mu_B$, respectively. Again, such small magnetic moments are explained by the large distance between Co layer and MoS₂. The electronic structures calculated for the considered systems also do not support their formation in the experiment: for MoS₂/gr/CoS_x/Co(0001) the linear dispersion of the graphene π band is partially restored with a clear n -doping of a graphene layer, which is opposite to the experimental observation, and the exchange spin-splitting of the MoS₂ bands is absent; for the gr/MoS₂/CoS_x/Co(0001) system the free-standing-like band structure of

MoS₂ is completely destroyed also indicating the strong hybridization of the electronic states at the MoS₂/CoS_x/Co(0001) interface.

The previous results presented in Fig. 4(a-d) indicate that in order to correctly theoretically reproduce the experimentally observed electronic structure of the considered system, the top-placed MoS₂/gr stack has to be electronically decoupled from the underlying Co(0001) surface by a layer of intercalated sulphur atoms. Following this point, on the next step the electronic and magnetic properties of the MoS₂/gr/S^{int}/Co(0001) and gr/MoS₂/S^{int}/Co(0001) systems were analyzed (Fig. 2(e,f) and Fig. 4(e,f)). Due to the decoupling of the MoS₂/gr stacks from the Co(0001) surface by the layer of S-atoms, the total energies for both systems are very close to each other with a difference of only ≈ 0.7 eV (or ≈ 0.9 meV per atom) in a slight favour of the former system (Tab. 2). This fact points to the equal probability for both stacks to be present in the formed and experimentally studied samples.

The adsorption of S-atoms at the interface between Co(0001) and MoS₂/gr stack drastically reduces the magnetic moment of Co interface atoms to $1.433 \mu_B$ compared to values for previously considered systems and value of $1.579 \mu_B$ for Co bulk (Tab. 2). This correlates with previous spectroscopic studies pointing to the formation of the so-called “dead” magnetic layer after adsorption of S on ferromagnetic surfaces with the reduction of the magnetic moment for surface atoms.^{43–45} The obtained bands dispersions of the graphene π and MoS₂ bands for MoS₂/gr/S^{int}/Co(0001) and gr/MoS₂/S^{int}/Co(0001) systems resemble the experimental data. In both systems graphene is *p*-doped with the position of the Dirac point at $E - E_F = 0.315$ eV and $E - E_F = 0.17$ eV for the former and later systems, respectively. At the same time the free-standing-like dispersion of electronic bands for MoS₂ is fully restored and reproduces the experimentally observed picture. However, the calculated band structures show the absence of any exchange spin-splitting for the MoS₂ bands in whole Brillouin zone disproving the previously published experimental and theoretical data. The calculated magnetic moment of $0.000 \mu_B$ for Mo and S atoms of the MoS₂ layer

in $\text{MoS}_2/\text{gr}/\text{S}^{\text{int}}/\text{Co}(0001)$ and $\text{gr}/\text{MoS}_2/\text{S}^{\text{int}}/\text{Co}(0001)$ also confirms the presently obtained results on the absence of any magnetic states in MoS_2 . These results are clearly understood by the large Co-Mo and Co-S distances of $[9.817]/[6.402]$ Å and $[8.261]/[4.845]$ Å for the $[\text{MoS}_2/\text{gr}]/[\text{gr}/\text{MoS}_2]$ stacks, respectively, adsorbed on $\text{S}/\text{Co}(0001)$, thus preventing the appearance of any ferromagnetic order in MoS_2 .

Conclusion

The recent experiments claim on the observation of the exchange spin-splitting of ≈ 20 meV for the MoS_2 bands at the Γ point in the $\text{MoS}_2/\text{gr}/\text{Co}(0001)$ system explaining this effect by the proximity effect from the gr/Co substrate. In the present work we performed the most realistic DFT studies of electronic and magnetic properties of different MoS_2/gr stacks on $\text{Co}(0001)$ taking into account the possible S intercalation at the gr/Co interface originating from the preparation procedure for the studied system. During these calculations several factors support the correctness of the employed computational approach in our work for the description of the studied system and we conclude that the $\text{MoS}_2/\text{gr}/\text{S}^{\text{int}}/\text{Co}(0001)$ stack has to be used for the modelling of the experimentally observed band structure (linear dispersion of the graphene π band with position of the Dirac point at $E - E_F \approx 0.3$ eV and free-standing-like dispersion of electronic bands for MoS_2 , see Tab. 3). However, opposite to the claimed experimentally observed exchange spin-splitting for the MoS_2 bands at the Γ point, our realistic large-scale calculations do not show any exchange splitting for the MoS_2 bands over the whole Brillouin zone pointing to the absence of any proximity effect for the MoS_2 layer in such system. Moreover, other systems which do not include the intercalated S layer or with MoS_2 in close vicinity to $\text{Co}(0001)$ also show vanishingly small (if any) exchange spin-splitting for the discussed band and magnetic moments of Mo and S atoms. The absence of any proximity effect is clearly explained by the van der Waals nature of interaction between layers at the relatively large distance between $\text{Co}(0001)$ and MoS_2 and by the screening

effect caused by a graphene layer. Therefore, we conclude that the present state-of-the-art calculations fully and correctly describe considered experimentally realized MoS₂/graphene stacks on the Co(0001) substrate, pointing to the importance of the correct modelling of the studied systems and correct application of theoretical methods. Moreover, our findings keep open the validity of the recent experimental observations and limited theoretical approaches used for the description of the studied systems. The present results also question the ability to manipulate the magnetic state of TMD MoS₂ in the proposed way via its decoupling from ferromagnetic substrate using graphene.

Methods

DFT calculations based on plane-wave basis sets of 400 eV cut-off energy were performed with the Vienna *ab initio* simulation package (VASP).^{46,47} The Perdew-Burke-Ernzerhof (PBE) exchange-correlation functional⁴⁸ was employed. The electron-ion interaction was described within the projector augmented wave (PAW) method⁴⁹ with C ($2s, 2p$), Co ($3d, 4s$), Mo ($4d, 5s$), and S ($3s, 3p$) states treated as valence states. The Brillouin-zone integration was performed on Γ -centered symmetry reduced Monkhorst-Pack mesh using a Methfessel-Paxton smearing method of first order with $\sigma = 0.15$ eV, except for the calculations of total energies. For those calculations, the tetrahedron method with Blöchl corrections⁵⁰ was used. The k -mesh for sampling the supercell Brillouin zone is chosen to be $6 \times 6 \times 1$. Dispersion interactions were considered by adding a $1/r^6$ atom-atom term as parameterized by Grimme (“D2” parameterization).⁵¹ The spin-orbit interaction is taken into account.

The supercells used in this work are presented in Figure 2. They are constructed from a slab of five layers of Co, a graphene and MoS₂ layers adsorbed on one (top) side of a metal slab and a vacuum region of at least 20.6 Å. The positions (x, y, z -coordinates) of C atoms, the ions of alloy (CoS_{*x*}), or intercalant (S^{int}) as well as z -coordinates of the two topmost layers of a substrate were fully relaxed until forces became smaller than 0.02 eV Å⁻¹. The

lattice constant in the lateral plane was set according to the optimized value of the bulk Co (2.488 Å). The supercells have a (9×9) lateral periodicity with respect to graphene and Co(0001) and a (7×7) lateral periodicity with respect to MoS₂. This way the lattice mismatch of both two-dimensional materials, graphene and MoS₂, is less than 1%. The bottom side of the slab was protected by a layer of Al atoms.^{35,36} Our test calculations for the (4×4) MoS₂/ (5×5) graphene/Co(0001) with the distances reported by Voroshnin et al.²⁷ with and without Al-passivation allow us to conclude that the claimed spin-splitting of the MoS₂-derived states at the Γ point is an artefact due to the wrong computational approach (Fig. 5). In order to simulate formation of CoS_x layer at the interface between the MoS₂-graphene heterostructure and the substrate, 20 Co atoms were randomly substituted by S atoms (Fig. 2(c,d)). In the structures presented in Figure 2(e,f), the interface S-layer consists of 25 atoms uniformly distributed between the Co surface and the adsorbed heterostructure. The optimized structures (x, y, z -coordinates) can be found in the Supporting Information.

The band structures calculated for the studied systems were unfolded to the graphene (1×1) and the MoS₂ (1×1) primitive unit cells according to the procedure described in Refs. 52,53 with the code BandUP.

Acknowledgement

The authors thank the National Natural Science Foundation of China (Grant No. 22272104) for financial support. E.V. and B.P. gratefully acknowledge the computing time granted by the Resource Allocation Board and provided on the supercomputer Lise and Emmy at NHR@ZIB and NHR@Göttingen as part of the NHR infrastructure. The calculations for this research were conducted with computing resources under the project bec00256.

Supporting Information Available

The following files are available free of charge.

- Structural data for MoS₂/gr/Co(0001) (TXT)
- Structural data for gr/MoS₂/Co(0001) (TXT)
- Structural data for MoS₂/gr/CoS_x/Co(0001) (TXT)
- Structural data for gr/MoS₂/CoS_x/Co(0001) (TXT)
- Structural data for MoS₂/gr/S^{int}/Co(0001) (TXT)
- Structural data for gr/MoS₂/S^{int}/Co(0001) (TXT)

References

1. Manzeli, S.; Ovchinnikov, D.; Pasquier, D.; Yazyev, O. V.; Kis, A. 2D Transition Metal Dichalcogenides. *Nat. Rev. Mater.* **2017**, *2*, 17033.
2. Helveg, S.; Lauritsen, J. V.; Lægsgaard, E.; Stensgaard, I.; Nørskov, J. K.; Clausen, B. S.; Topsøe, H.; Besenbacher, F. Atomic-Scale Structure of Single-Layer MoS₂ Nanoclusters. *Phys. Rev. Lett.* **1999**, *84*, 951–954.
3. Chianelli, R. R.; Siadati, M. H.; Rosa, M. P. D. I.; Berhault, G.; Wilcoxon, J. P.; Bearden, R.; Abrams, B. L. Catalytic Properties of Single Layers of Transition Metal Sulfide Catalytic Materials. *Catal. Rev.* **2006**, *48*, 1–41.
4. Tumino, F.; Casari, C. S.; Bassi, A. L.; Tosoni, S. Nature of Point Defects in Single-Layer MoS₂ Supported on Au(111). *J. Phys. Chem. C* **2020**, *124*, 12424–12431.
5. Splendiani, A.; Sun, L.; Zhang, Y.; Li, T.; Kim, J.; Chim, C.-Y.; Galli, G.; Wang, F. Emerging Photoluminescence in Monolayer MoS₂. *Nano Lett.* **2010**, *10*, 1271–1275.
6. Mak, K. F.; Lee, C.; Hone, J.; Shan, J.; Heinz, T. F. Atomically Thin MoS₂: A New Direct-Gap Semiconductor. *Phys. Rev. Lett.* **2010**, *105*, 136805.

7. Fan, X.; Singh, D. J.; Zheng, W. Valence Band Splitting on Multilayer MoS₂: Mixing of Spin-Orbit Coupling and Interlayer Coupling. *J. Phys. Chem. Lett.* **2016**, *7*, 2175–2181.
8. Cao, T.; Wang, G.; Han, W.; Ye, H.; Zhu, C.; Shi, J.; Niu, Q.; Tan, P.; Wang, E.; Liu, B.; Feng, J. Valley-Selective Circular Dichroism of Monolayer Molybdenum Disulphide. *Nat. Commun.* **2012**, *3*, 887.
9. Xiao, D.; Liu, G.-B.; Feng, W.; Xu, X.; Yao, W. Coupled Spin and Valley Physics in Monolayers of MoS₂ and Other Group-VI Dichalcogenides. *Phys. Rev. Lett.* **2012**, *108*, 196802.
10. Alidoust, N.; Bian, G.; Xu, S.-Y.; Sankar, R.; Neupane, M.; Liu, C.; Belopolski, I.; Qu, D.-X.; Denlinger, J. D.; Chou, F.-C.; Hasan, M. Z. Observation of Monolayer Valence Band Spin-Orbit Effect and Induced Quantum Well States in MoX₂. *Nat. Commun.* **2014**, *5*, 4673.
11. Suzuki, R.; Sakano, M.; Zhang, Y. J.; Akashi, R.; Morikawa, D.; Harasawa, A.; Yaji, K.; Kuroda, K.; Miyamoto, K.; Okuda, T.; Ishizaka, K.; Arita, R.; Iwasa, Y. Valley-Dependent Spin Polarization in Bulk MoS₂ With Broken Inversion Symmetry. *Nat. Nanotechnol.* **2014**, *9*, 611–617.
12. Bana, H.; Travaglia, E.; Bignardi, L.; Lacovig, P.; Sanders, C. E.; Dendzik, M.; Michiardi, M.; Bianchi, M.; Lizzit, D.; Presel, F.; Angelis, D. D.; Apostol, N.; Das, P. K.; Fujii, J.; Vobornik, I.; Larciprete, R.; Baraldi, A.; Hofmann, P.; Lizzit, S. Epitaxial Growth of Single-Orientation High-Quality MoS₂ Monolayers. *2D Mater.* **2018**, *5*, 035012.
13. Aivazian, G.; Gong, Z.; Jones, A. M.; Chu, R.-L.; Yan, J.; Mandrus, D. G.; Zhang, C.; Cobden, D.; Yao, W.; Xu, X. Magnetic Control of Valley Pseudospin in Monolayer WSe₂. *Nat. Phys.* **2015**, *11*, 148–152.

14. Slobodeniuk, A. O.; Basko, D. M. Spin-Flip Processes and Radiative Decay of Dark Intravalley Excitons in Transition Metal Dichalcogenide Monolayers. *2D Mater.* **2016**, *3*, 035009.
15. Robert, C.; Han, B.; Kapuscinski, P.; Delhomme, A.; Faugeras, C.; Amand, T.; Molas, M. R.; Bartos, M.; Watanabe, K.; Taniguchi, T.; Urbaszek, B.; Potemski, M.; Marie, X. Measurement of the Spin-Forbidden Dark Excitons in MoS₂ and MoSe₂ Monolayers. *Nat. Commun.* **2020**, *11*, 4037.
16. Huang, M.; Xiang, J.; Feng, C.; Huang, H.; Liu, P.; Wu, Y.; N'Diaye, A. T.; Chen, G.; Liang, J.; Yang, H.; Liang, J.; Cui, X.; Zhang, J.; Lu, Y.; Liu, K.; Hou, D.; Liu, L.; Xiang, B. Direct Evidence of Spin Transfer Torque on Two-Dimensional Cobalt-Doped MoS₂ Ferromagnetic Material. *ACS Appl. Electron. Mater.* **2020**, *2*, 1497–1504.
17. Fu, S.; Kang, K.; Shayan, K.; Yoshimura, A.; Dadras, S.; Wang, X.; Zhang, L.; Chen, S.; Liu, N.; Jindal, A.; Li, X.; Pasupathy, A. N.; Vamivakas, A. N.; Meunier, V.; Strauf, S.; Yang, E.-H. Enabling Room Temperature Ferromagnetism in Monolayer MoS₂ Via In Situ Iron-Doping. *Nat. Commun.* **2020**, *11*, 2034.
18. Cai, L.; He, J.; Liu, Q.; Yao, T.; Chen, L.; Yan, W.; Hu, F.; Jiang, Y.; Zhao, Y.; Hu, T.; Sun, Z.; Wei, S. Vacancy-Induced Ferromagnetism of MoS₂ Nanosheets. *J. Am. Chem. Soc.* **2015**, *137*, 2622–2627.
19. Jia, C.; Zhou, B.; Song, Q.; Zhang, X.; Jiang, Z. Modulating the Magnetic Properties of MoS₂ Monolayers by Group VIII Doping and Vacancy Engineering. *RSC Adv.* **2018**, *8*, 18837–18850.
20. Tsai, S.; Yang, C.; Lee, C.; Lu, L.; Liang, H.; Lin, J.; Yu, Y.; Chen, C.; Chung, T.; Kaun, C.; Hsu, H.; Huang, S.; Chang, W.; He, L.; Lai, C.; Wang, K. L. Room-Temperature Ferromagnetism of Single-Layer MoS₂ Induced by Antiferromagnetic Proximity of Yttrium Iron Garnet. *Adv. Quantum Technol.* **2021**, *4*, 2000104.

21. Bragança, H.; Zeng, H.; Dias, A. C.; Correa, J. H.; Qu, F. Magnetic-Gateable Valley Exciton Emission. *npj Comput. Mater.* **2020**, *6*, 90.
22. Tu, Z.; Zhou, T.; Ersevimi, T.; Arachchige, H. S.; Hanbicki, A. T.; Friedman, A. L.; Mandrus, D.; Ouyang, M.; Žutić, I.; Gong, C. Spin-Orbit Coupling Proximity Effect in MoS₂/Fe₃GeTe₂ Heterostructures. *Appl. Phys. Lett.* **2022**, *120*, 043102.
23. Krane, N.; Lotze, C.; Bogdanoff, N.; Reecht, G.; Zhang, L.; Briseno, A. L.; Franke, K. J. Mapping the Perturbation Potential of Metallic and Dipolar Tips in Tunneling Spectroscopy on MoS₂. *Phys. Rev. B* **2019**, *100*, 035410.
24. Trishin, S.; Lotze, C.; Bogdanoff, N.; Oppen, F. v.; Franke, K. J. Moiré Tuning of Spin Excitations: Individual Fe Atoms on MoS₂/Au(111). *Phys. Rev. Lett.* **2021**, *127*, 236801.
25. Li, T.; Guo, W.; Ma, L.; Li, W.; Yu, Z.; Han, Z.; Gao, S.; Liu, L.; Fan, D.; Wang, Z.; Yang, Y.; Lin, W.; Luo, Z.; Chen, X.; Dai, N.; Tu, X.; Pan, D.; Yao, Y.; Wang, P.; Nie, Y. *et al.* Epitaxial Growth of Wafer-Scale Molybdenum Disulfide Semiconductor Single Crystals on Sapphire. *Nat. Nanotechnol.* **2021**, *16*, 1201–1207.
26. Ehlen, N.; Hall, J.; Senkovskiy, B. V.; Hell, M.; Li, J.; Herman, A.; Smirnov, D.; Fedorov, A.; Voroshnin, V. Y.; Santo, G. D.; Petaccia, L.; Michely, T.; Grüneis, A. Narrow Photoluminescence and Raman Peaks of Epitaxial MoS₂ on Graphene/Ir(111). *2D Mater.* **2018**, *6*, 011006.
27. Voroshnin, V.; Tarasov, A. V.; Bokai, K. A.; Chikina, A.; Senkovskiy, B. V.; Ehlen, N.; Usachov, D. Y.; Gruneis, A.; Krivenkov, M.; Sanchez-Barriga, J.; Fedorov, A. Direct Spectroscopic Evidence of Magnetic Proximity Effect in MoS₂ Monolayer on Graphene/Co. *ACS Nano* **2022**, *16*, 7448–7456.
28. Himpsel, F. Correlation Between Magnetic Splitting and Magnetic Moment for 3d Transition Metals. *J. Magn. Magn. Mater.* **1991**, *102*, 261–265.

29. Himpsel, F. J.; Ortega, J. E.; Mankey, G. J.; Willis, R. F. Magnetic Nanostructures. *Adv. Phys.* **1998**, *47*, 511–597.
30. Weser, M.; Rehder, Y.; Horn, K.; Sicot, M.; Fonin, M.; Preobrajenski, A. B.; Voloshina, E. N.; Goering, E.; Dedkov, Y. S. Induced Magnetism of Carbon Atoms at the Graphene/Ni(111) Interface. *Appl. Phys. Lett.* **2010**, *96*, 012504.
31. Mertins, H.-C.; Valencia, S.; Gudat, W.; Oppeneer, P. M.; Zaharko, O.; Grimmer, H. Direct Observation of Local Ferromagnetism on Carbon in Multilayers. *Europhys. Lett.* **2004**, *66*, 743–748.
32. Mertins, H.-C.; Jansing, C.; Gilbert, M.; Krivenkov, M.; Sanchez-Barriga, J.; Varykhalov, A.; Rader, O.; Wahab, H.; Timmers, H.; Gaupp, A.; Tesch, M.; Sokolov, A.; Legut, D.; Oppeneer, P. M. Magneto-Optical Reflection Spectroscopy on Graphene/Co in the Soft X-Ray Range. *J. Phys. Conf. Ser.* **2017**, *903*, 012025.
33. Rader, O.; Varykhalov, A.; Sanchez-Barriga, J.; Marchenko, D.; Rybkin, A.; Shikin, A. M. Is There a Rashba Effect in Graphene on 3d Ferromagnets? *Phys. Rev. Lett.* **2009**, *102*, 057602.
34. Iwasawa, H. High-Resolution Angle-Resolved Photoemission Spectroscopy and Microscopy. *Electron. Struct.* **2020**, *2*, 043001.
35. Li, Z.; Gong, S.; Yang, Z. Large Spin-Orbit Splitting of Surface States in Ultrathin Au (111) Films. *Phys. Lett. A*, **2021**, *377*, 129–132.
36. Voloshina, E.; Dedkov, Y. Realistic Large-Scale Modeling of Rashba and Induced Spin-Orbit Effects in Graphene/High-Z-Metal System. *Adv. Theory Simul.*, **2018**, *1*, 1800063.
37. Voloshina, E.; Dedkov, Y. In *Electronic and Magnetic Properties of the Graphene-Ferromagnet Interfaces: Theory vs. Experiment*; Mikhailov, S., Ed.; Physics and Applications of Graphene - Experiments; InTech, 2011; pp 329 – 351.

38. Khomyakov, P. A.; Giovannetti, G.; Rusu, P. C.; Brocks, G.; Brink, J. v. d.; Kelly, P. J. First-Principles Study of the Interaction and Charge Transfer Between Graphene and Metals. *Phys. Rev. B* **2009**, *79*, 195425.
39. Yue, W.; Guo, Q.; Dedkov, Y.; Voloshina, E. Electronic and Magnetic Properties of the Graphene/Y/Co(0001) Interfaces: Insights from the Density Functional Theory Analysis. *ACS Omega* **2022**, *7*, 7304–7310.
40. Usachov, D.; Fedorov, A.; Otrokov, M. M.; Chikina, A.; Vilkov, O.; Petukhov, A.; Rybkin, A. G.; Koroteev, Y. M.; Chulkov, E. V.; Adamchuk, V. K.; Grüneis, A.; Laubschat, C.; Vyalikh, D. V. Observation of Single-Spin Dirac Fermions at the Graphene/Ferromagnet Interface. *Nano Lett.* **2015**, *15*, 2396–2401.
41. Batzill, M. The Surface Science of Graphene: Metal Interfaces, CVD Synthesis, Nanoribbons, Chemical Modifications, and Defects. *Surf. Sci. Rep.* **2012**, *67*, 83–115.
42. Dedkov, Y.; Voloshina, E. Graphene Growth and Properties on Metal Substrates. *J. Phys. Condens. Matter* **2015**, *27*, 303002.
43. Göpel, W. “Magnetic Dead Layers” on Chemisorption at Ferromagnetic Surfaces. *Surf. Sci.* **1979**, *85*, 400–412.
44. Schmitt, W.; Hopster, H.; Güntherodt, G. Influence of Adsorbates on Surface Magnetism Studied by Spin-Resolved Photoemission Spectroscopy. *Phys. Rev. B* **1984**, *31*, 4035–4038.
45. Schmitt, W.; Kämper, K.-P.; Güntherodt, G. Effect of Adsorbates on the Spin-Polarized Photoemission of Itinerant Ferromagnets. *Phys. Rev. B* **1987**, *36*, 3763–3768.
46. Kresse, G.; Furthmüller, J. Efficient Iterative Schemes for Ab Initio Total-Energy Calculations Using a Plane-Wave Basis Set. *Phys. Rev. B* **1996**, *54*, 11169–11186.

47. Kresse, G.; Joubert, D. From Ultrasoft Pseudopotentials to the Projector Augmented-Wave Method. *Phys. Rev. B* **1999**, *59*, 1758–1775.
48. Perdew, J. P.; Burke, K.; Ernzerhof, M. Generalized Gradient Approximation Made Simple. *Phys. Rev. Lett.* **1996**, *77*, 3865–3868.
49. Blöchl, P. E. Projector Augmented-Wave Method. *Phys. Rev. B* **1994**, *50*, 17953–17979.
50. Blöchl, P. E.; Jepsen, O.; Andersen, O. K. Improved Tetrahedron Method for Brillouin-Zone Integrations. *Phys. Rev. B* **1994**, *49*, 16223–16233.
51. Grimme, S. Semiempirical GGA-Type Density Functional Constructed With a Long-Range Dispersion Correction. *J. Comput. Chem.* **2006**, *27*, 1787–1799.
52. Medeiros, P. V. C.; Stafström, S.; Björk, J. Effects of Extrinsic and Intrinsic Perturbations on the Electronic Structure of Graphene: Retaining an Effective Primitive Cell Band Structure by Band Unfolding. *Phys. Rev. B* **2014**, *89*, 041407.
53. Medeiros, P. V. C.; Tsirkin, S. S.; Stafström, S.; Björk, J. Unfolding Spinor Wave Functions and Expectation Values of General Operators: Introducing the Unfolding-Density Operator. *Phys. Rev. B* **2015**, *91*, 041116.

Table 1: Magnetic moments of C and Co (in μ_B) obtained for the bulk Co, Co(0001) surface and gr/Co(0001) interface.

	bulk Co	Co(0001)	gr/Co
$m(\text{C1})$	–	–	–0.042
$m(\text{C2})$	–	–	0.038
$m(\text{Co1})$	–	1.707	1.514
$m(\text{Co2})$	–	1.616	1.574
$m(\text{Co3})$	1.616	1.578	1.579

Table 2: Results for the MoS₂-graphene heterostructures on ferromagnetic Co(0001): total energy (E_{tot} , in eV per unit cell); the mean distances between different layers in the optimized structures (for details, see Fig. 2: $d(\text{gr-S1})$, $d(\text{gr-Co})$, $d(\text{S1-Co})$, $d(\text{Mo-Co})$, $d(\text{gr-S}^{\text{int}})$, $d(\text{S1-S}^{\text{int}})$, in Å); corrugation of the graphene layer (gr-corr., in Å); average magnetic moments of Mo, S, C, and Co ($m(\text{Mo})$, $m(\text{S1})$, $m(\text{S2})$, $m(\text{S}^{\text{int}})$, $m(\text{C1})$, $m(\text{C2})$, $m(\text{Co1})$, $m(\text{Co2})$, $m(\text{Co3})$, in μ_{B} per atom).

	MoS ₂ /gr/ Co(0001)	gr/MoS ₂ / Co(0001)	MoS ₂ /gr/ CoS _x ^{int} /Co(0001)	gr/MoS ₂ / CoS _x ^{int} /Co(0001)	MoS ₂ /gr/ S ^{int} /Co(0001)	gr/MoS ₂ / S ^{int} /Co(0001)
E_{tot}	-5891.0957	-5900.1487	-5832.7294	-5843.6277	-6018.2870	-6017.5665
$d(\text{gr-S1})$	3.312	3.388	3.374	3.378	3.415	3.391
$d(\text{gr-Co})$	2.092	8.551	2.683	8.726	4.847	11.347
$d(\text{S1-Co})$	5.404	2.026	6.057	2.227	8.261	4.845
$d(\text{Mo-Co})$	6.960	3.618	7.611	3.799	9.817	6.402
$d(\text{gr-S}^{\text{int}})$	–	–	2.808	9.031	3.219	9.720
$d(\text{S1-S}^{\text{int}})$	–	–	6.182	2.532	6.634	3.219
gr-corr.	0.058	0.089	0.966	0.210	0.132	0.067
$m(\text{Mo})$	-0.002	-0.011	0.003	-0.007	0.000	0.000
$m(\text{S1})$	0.000	0.020	0.000	0.012	0.000	0.000
$m(\text{S2})$	0.000	0.003	0.000	0.001	0.000	0.000
$m(\text{S}^{\text{int}})$	–	–	0.057	0.031	0.009	0.009
$m(\text{C1})$	-0.042	-0.002	-0.015	-0.002	0.000	0.000
$m(\text{C2})$	0.038	0.001	0.017	0.001	0.000	0.000
$m(\text{Co1})$	1.503	1.520	1.509	1.316	1.433	1.433
$m(\text{Co2})$	1.558	1.633	1.570	1.519	1.585	1.586
$m(\text{Co3})$	1.559	1.586	1.588	1.594	1.589	1.589

Table 3: Comparison between the experimental observations and theoretical data for the six systems under study (“✓” - experimental observable is reproduced in calculations; “✗” - experimental observable is not reproduced in calculations).

Experimental observation	MoS ₂ /gr/ Co(0001)	gr/MoS ₂ / Co(0001)	MoS ₂ /gr/ CoS _x ^{int} /Co(0001)	gr/MoS ₂ / CoS _x ^{int} /Co(0001)	MoS ₂ /gr/ S ^{int} /Co(0001)	gr/MoS ₂ / S ^{int} /Co(0001)
gr- π linear dispersion	✗	✓	partially	✓	✓	✓
gr p -doping	✗	✗	✗	✗	✓	partially
freestanding MoS ₂	✓	✗	✓	✗	✓	✓

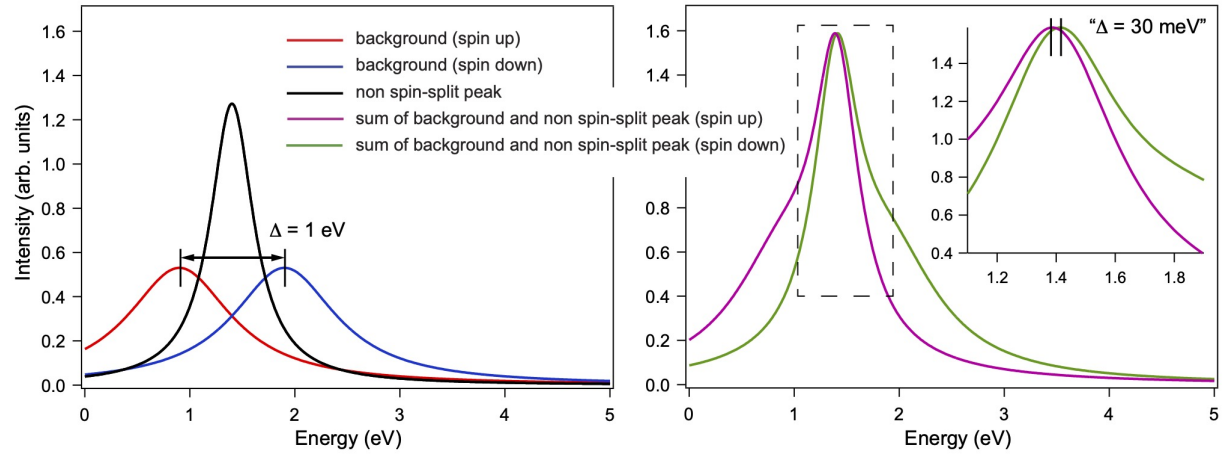


Figure 1: The formation of the “artificial” spin-polarization in the initially non spin-polarized peak by the spin-polarized photoemission background signal (for details see the text).

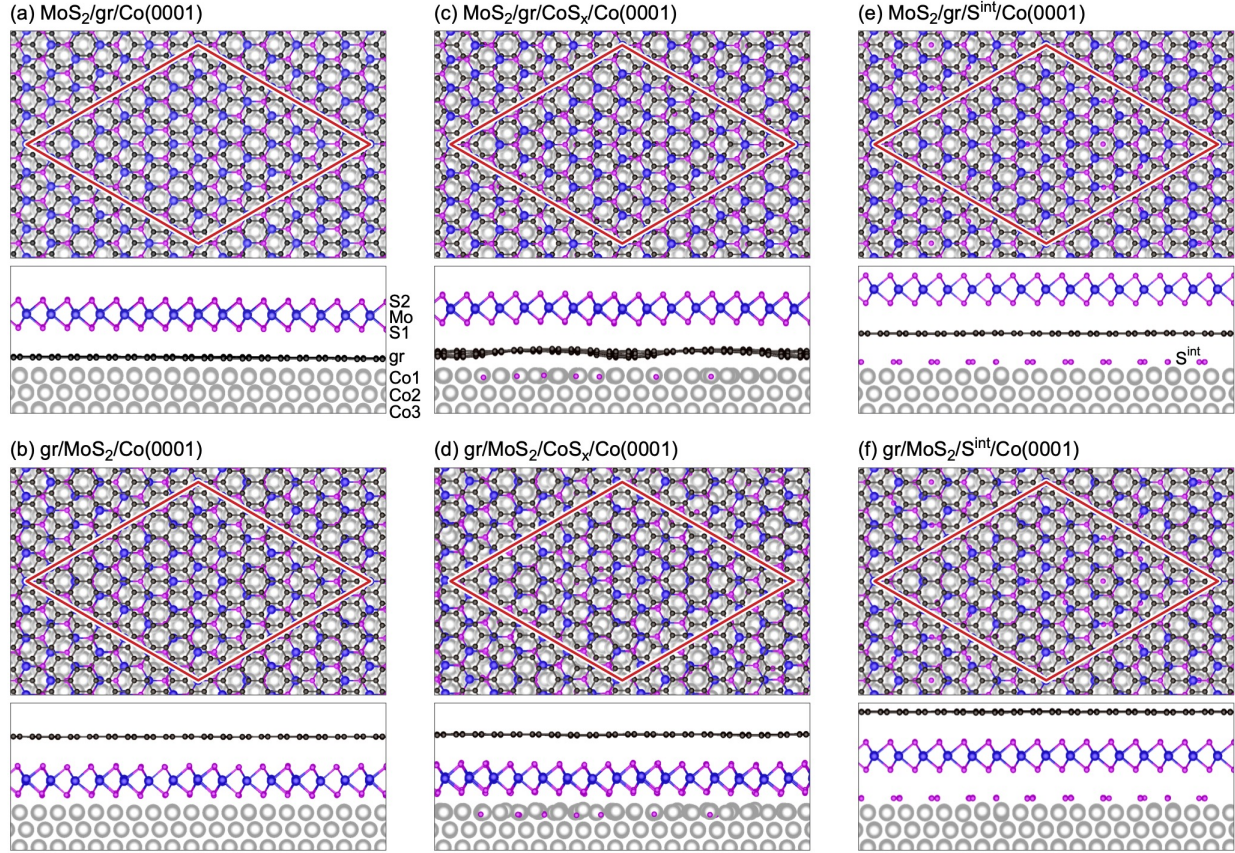


Figure 2: Optimized crystallographic structures (top and side views) of the MoS_2 -graphene heterostructures on ferromagnetic $\text{Co}(0001)$ considered in this work. The red rhombus marks the unit cell.

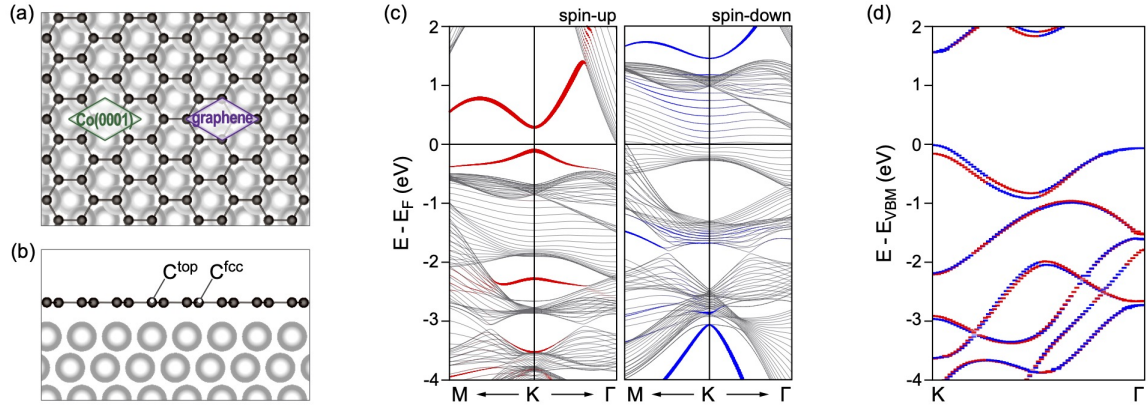


Figure 3: (a,b) Crystallographic structure of the lattice-matched graphene/Co(0001) interface: top (a) and side (b) views. (c) Spin-resolved band structure of graphene/Co(0001) in the vicinity of the K point. (d) Spin-resolved band structure of free-standing MoS₂. All visible spin-splittings are due to the spin-orbit interaction.

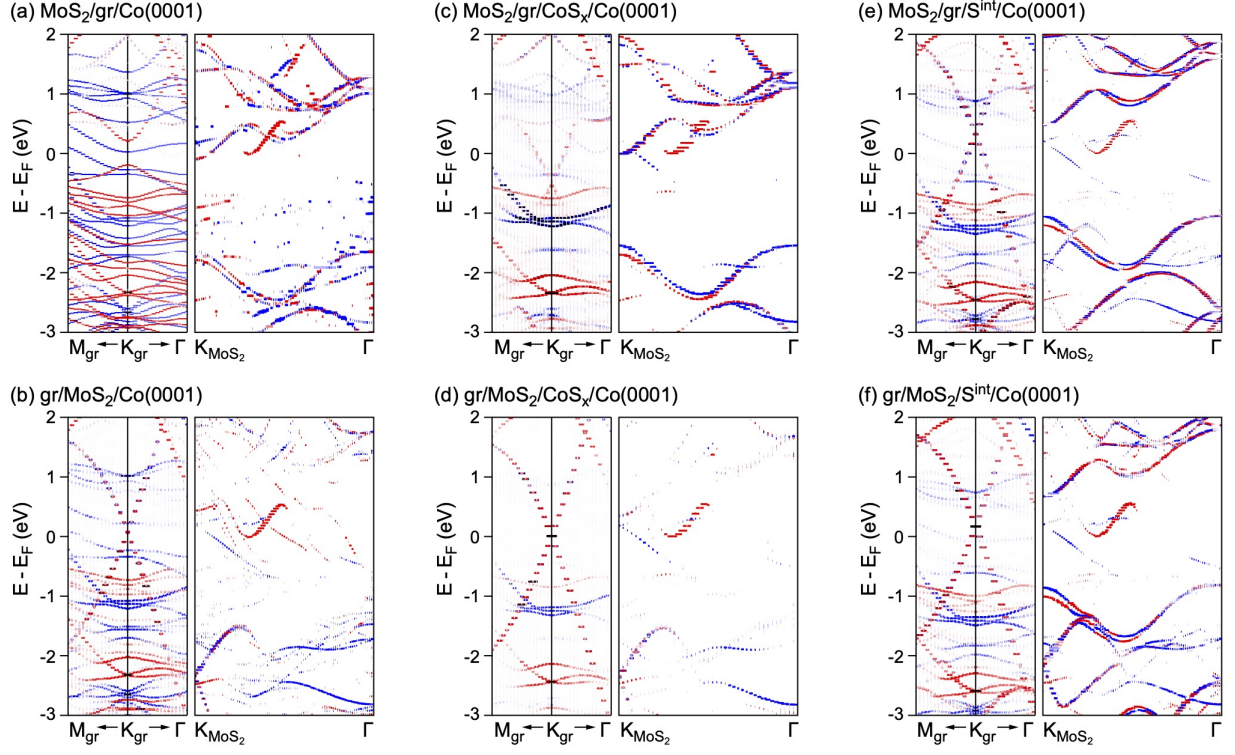


Figure 4: Spin-resolved band structures of the MoS₂-graphene heterostructures on ferromagnetic Co(0001) obtained after the unfolding procedure for the graphene (1×1) primitive cell (left) and MoS₂ (1×1) primitive cell (right). Size of the filled circles gives the number of primitive cell bands crossing particular (k, E) in the unfolding procedure, that is, the partial density of states at (k, E) for graphene (left) and MoS₂ (right), respectively.

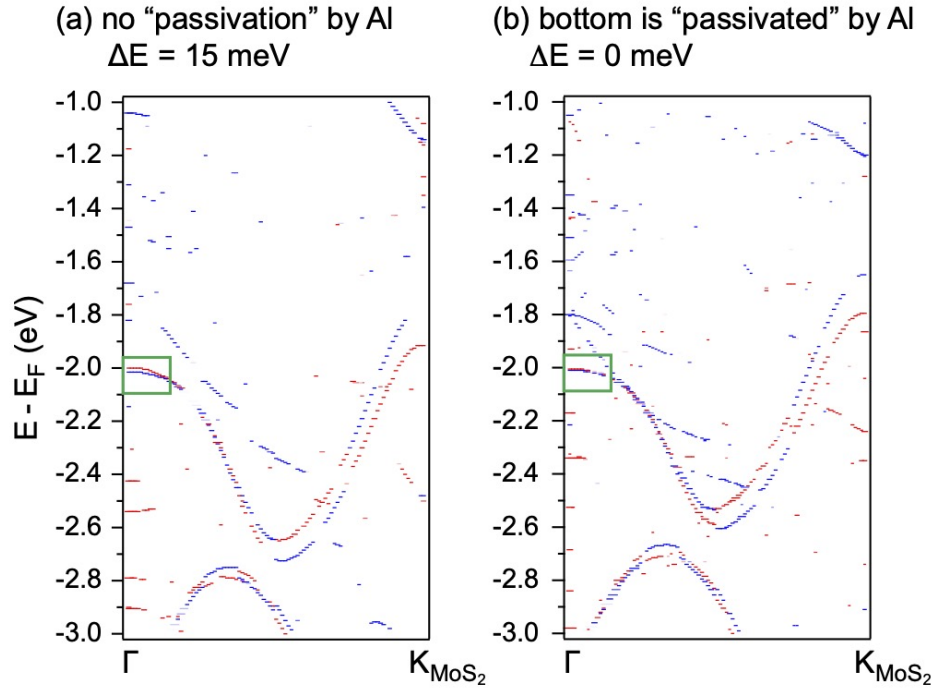


Figure 5: Effect of the bottom passivation of the $\text{MoS}_2/\text{gr}/\text{Co}(0001)$ slab by Al atoms: (a) no passivation by Al, with exchange splitting of the MoS_2 -derived states, (b) bottom is passivated by Al, without exchange splitting of the MoS_2 -derived states. The area of interest is marked by the green rectangle.